Supplementary Information

Self-propulsion of catalytic nanomotors synthesised by seeded growth of asymmetric platinum-gold nanoparticles

Ibon Santiago[a], Luyun Jiang[b], John Foord [b*] and Andrew J. Turberfield[a*]

[a] *Department of Physics, University of Oxford, Clarendon Laboratory, Parks Road, Oxford OX1 3PU, United Kingdom*

[b] *Department of Chemistry, University of Oxford , South Parks Road, Oxford, OX1 3TA, United Kingdom*

Methods/Experimental

M1 | Materials and reagents

Reagents were purchased from Sigma-Aldrich and are of A.C.S. reagent grade unless otherwise stated. All solutions and subsequent dilutions were prepared with Milli-Q water (>18 MΩ cm).

M2 | Chemical synthesis of Au-Pt NP

Pt-Au NP were synthesised by stirring 1 mL of monodisperse 15 nm Au nanoparticles (1.4×10^{12} particles/mL in 2mM sodium citrate, BBI) and 100 µl of K_2PtCl_4 (final concentration 0.1 mM) for 15 min, then slowly adding 20 µl 1mM $NaBH_4$ dropwise, while stirring, until a colour change from red to dark red occurred (SI Figure S2). A final K_2PtCl_4 concentration of 0.1mM corresponds to a Pt ion:Au atom ratio of 1:3. Where other K_2PtCl_4 concentrations are indicated in the text, all other quantities (including final volume) are unchanged.

M3 | Electrochemical measurements of catalytic activity

Electrochemical measurements were performed at room temperature (20±2ºC) with µ-AUTOLAB III potentiostat (Eco-Chemie, Netherlands) running GPES software. A three-

electrode system was used consisting of a Pt wire as counter electrode, an Ag/AgCl reference electrode, and a working electrode prepared by dropping 10 µl of 0.02 mg/L 10 nm Ag NP (0.01 mg/ml, Sigma-Aldrich) onto a 0.37 cm^2 glassy carbon surface (GCE). A rotating disk electrode (RDE) was used at a rotating speed of 1300 rpm. The potential was held at -0.6 V in solution containing 25 mM H_2O_2 and 0.1 M KCl. After the current baseline stabilised, a solution of catalyst particles was added. The current decreased linearly after few seconds, corresponding to the decomposition of H_2O_2 in solution (the calibration is shown in SI-Figure 5a). The catalytic activity was calculated from fitted slopes and the calibration using a catalase standard (SI-Figure 5b and c).

M4 | Characterisation of Pt-Au particles

The chemical composition of the particle surface was measured using X-ray photoelectron spectroscopy (XPS, VG Escalab with Al-K X-ray source). XPS energy spectra of ejected electrons were processed using CasaXPS software for peak fitting and identification.

Dynamic light scattering (DLS) measurements were carried out in a Zetasizer Nano (Malvern) with an instrument scattering angle of 173^0. As-prepared samples were diluted 8 times and were added to a 40µl-disposable plastic micro cuvette (ZEN0040) together with the appropriate amount of H_2O_2, resulting in the indicated final concentrations of H_2O_2. The sample was immediately loaded into the machine and 14 measurements of 10 s each were taken at 25^0C. This was repeated 3 times for each sample. The reported diffusion constants were computed from the intensity of the scattered light using the proprietary Malvern software package at its standard settings. The software uses cumulant analysis to extract mean diffusion coefficients D and distribution analysis to obtain diffusion-coefficient distribution curves from fitting measured intensity autocorrelation functions $g_2(t)$.

Particle morphology was analysed by TEM (FEI Tecnai 12 at 120 keV) and HAADF-STEM (JEOL ARM-200F equipped with EDX). Samples for TEM were prepared on carbon-coated Cu grids by drop-casting and evaporation.

SI- Figure 1 | UV-vis spectra for uncoated 15 nm Au NP, asymmetric Pt-Au NP (prepared with precursor K_2PtCl_4 concentration 0.1 mM) and approximately symmetric Pt-Au NP (with precursor K_2PtCl_4 1 mM). As Pt grows the characteristic Au plasmon resonance peak weakens.

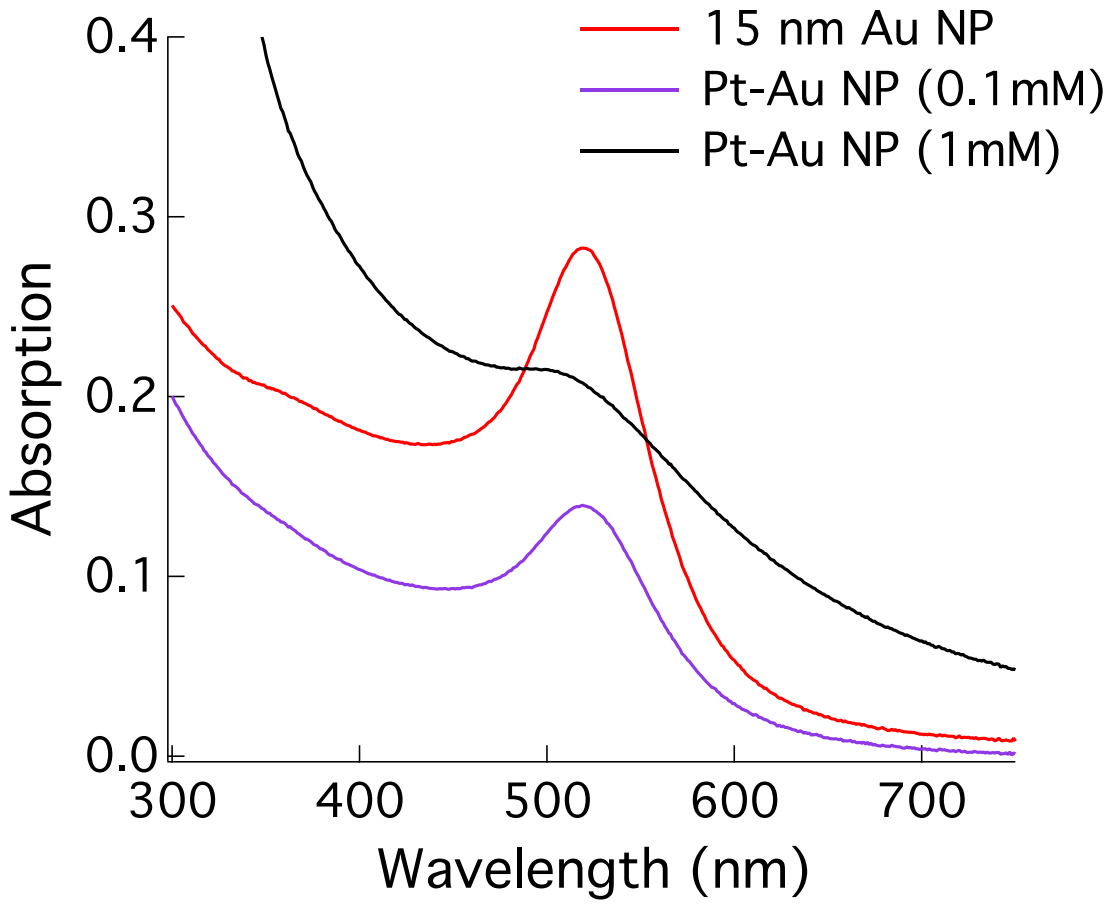

SI- Figure 2 | Platinum growth on Au NP. TEM micrographs and size distributions (hydrodynamic radius) measured by DLS of **(a)** 15 nm Au nanoparticles and **(b-c)** Pt-Au NP prepared with increasing concentrations of K_2PtCl_4 (**b** 0.1 mM, **c** 1mM and **d** 3mM). Scale bars: 50 nm.

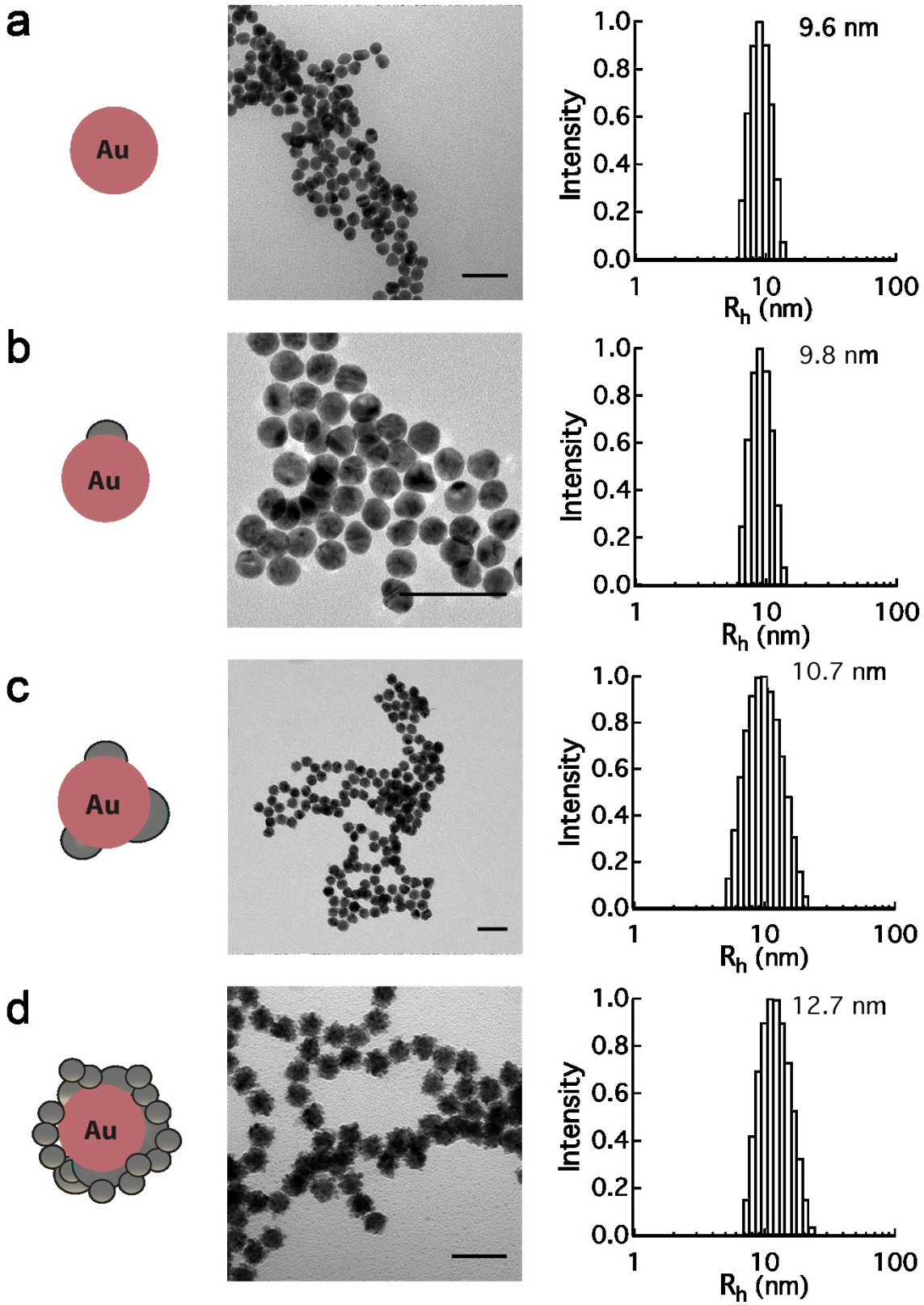

SI- Figure 3 | X-ray photoelectron spectroscopy (XPS) analysis of nanoparticle surface compositions for **(a)** 15 nm Au nanoparticles and **(b-d)** Pt-Au NP prepared using increasing initial concentrations of K_2PtCl_4 (**b** 0.1 mM, **c** 1 mM and **d** 3 mM). Grey lines represent the raw data; smooth solid and dashed lines are curve-fitting results.

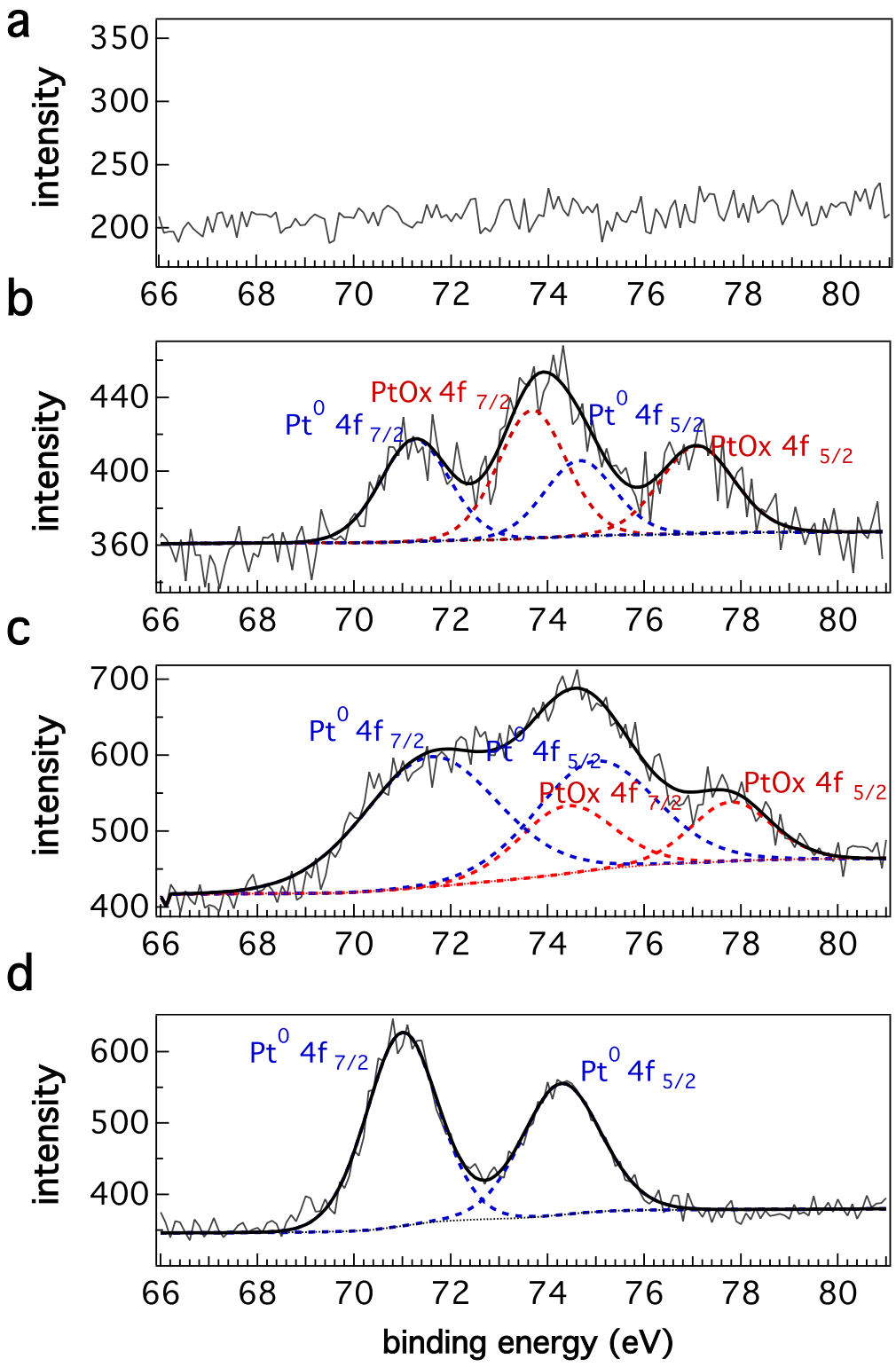

SI- Figure 4 | (**a,b**) TEM micrographs of unfiltered physical mixtures of reduced Pt (Pt precursor concentration of 3 mM) and Au NP. Reduced Pt and unchanged Au NP can be distinguished. (**c,d**) TEM micrographs of asymmetric Pt-Au NP with distinguishable Pt clusters (precursor concentration 0.1 mM). Scale bars: 20 nm.

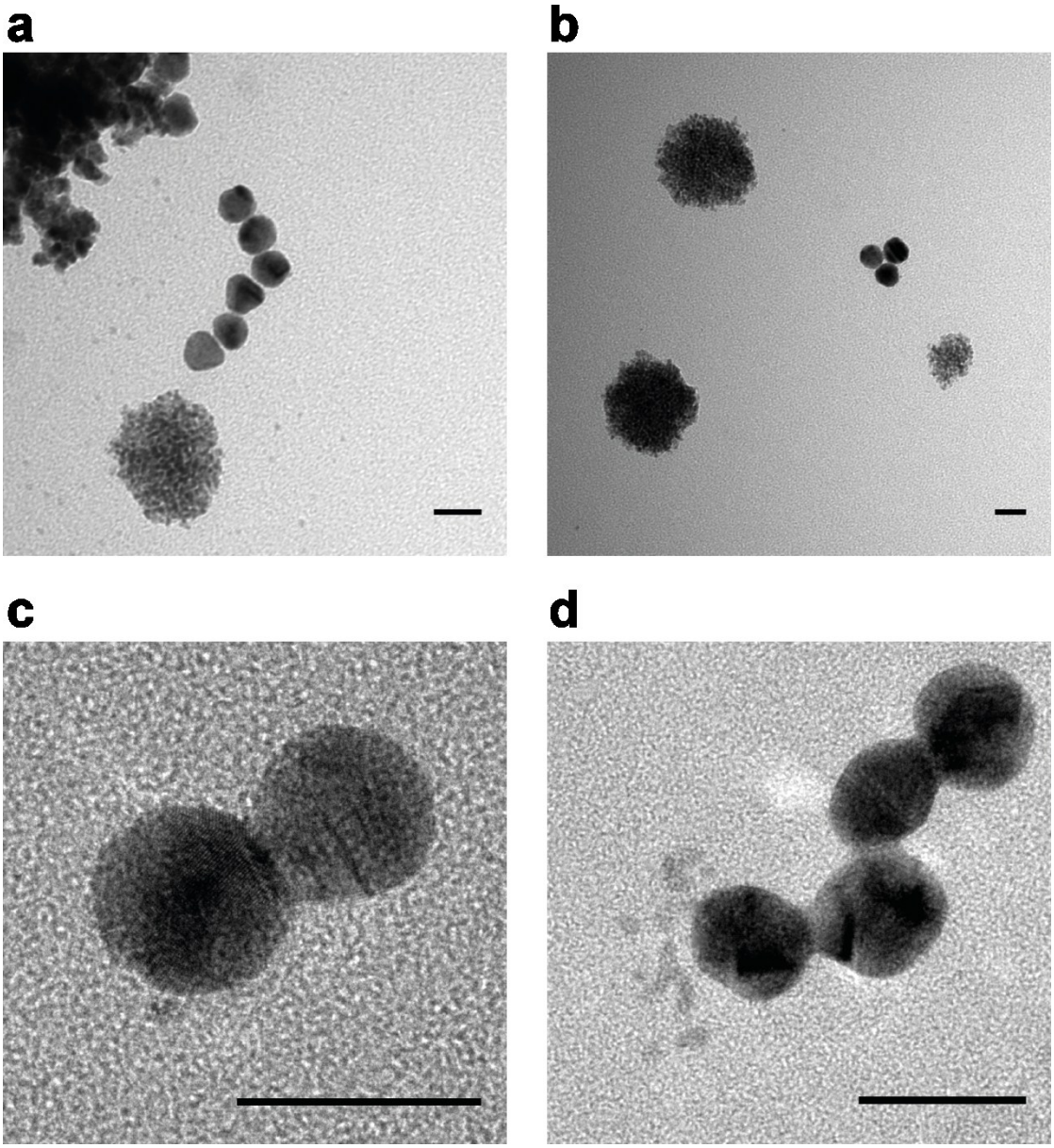

SI- Figure 5 | Electrochemical characterisation of the catalytic activity of Pt-Au NP. A Ag-coated glassy carbon electrode, prepared by dropping 10 µl of 0.02 mg/L 10 nm Ag NP onto a 0.37 cm^2 glassy carbon surface, was used as a H_2O_2 sensor. **(a)** Amperometric response of the H_2O_2 sensor at a constant potential of -0.6 V vs. Ag/AgCl in 0.1 M KCl solution with successive additions of H_2O_2. Insert: cathodic peak current vs. H_2O_2 concentration, with a slope of 4.63 mM/µA. **(b)** Amperometric response after successive additions of 10 µL 15 nm Au NP, control solution (reduced Pt physically mixed with Au NP; Pt precursor concentration 0.1 mM) and asymmetric Pt-Au NP (Pt precursor concentration 0.1 mM) into 25 mM H_2O_2. **(c)** Decrease of $[H_2O_2]$ after addition of various concentrations of 5 nm Pt NPs (from 78 pM to 1.5 nM, see insert). Insert: initial H_2O_2 decomposition rate vs. Pt NP concentration. **(d)** Decrease of $[H_2O_2]$ after addition of various concentrations of catalase (from 64 to 510 pM, see insert). Insert: initial H_2O_2 decomposition rate vs. catalase concentration. Measurements with both Pt NP and catalase show a linear relationship between catalyst concentration and slope (change of H_2O_2 over time) for low catalytic activities (slope < 0.08 mM/s). Using catalase as a cross-calibration standard (rate = 100%), a catalytic rate of 2.5% was measured for an equivalent particle concentration of asymmetric Pt-Au NP, 7.4% for thick layer core-shell Pt-Au NP (Pt precursor concentration 3 mM) and 0.29% for the control solution.

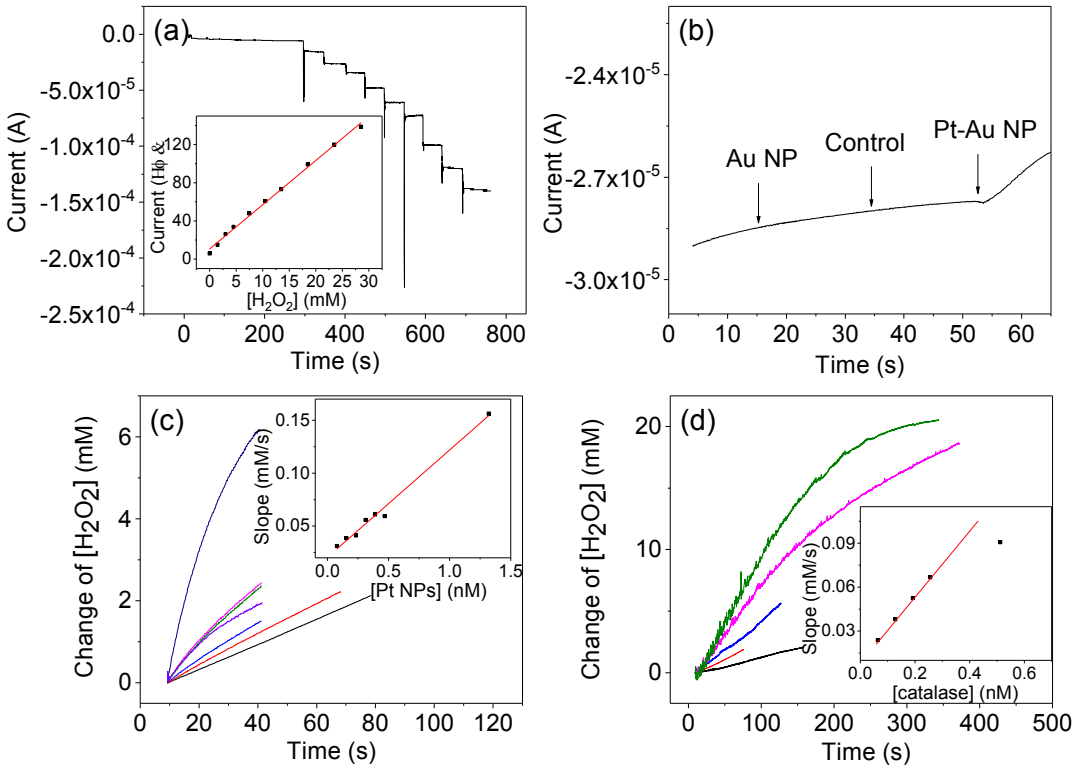

SI- Figure 6 | Distributions of asymmetric Pt-Au NP diffusion coefficients inferred from DLS with increasing concentrations of H_2O_2 **(a)** in water and **(b)** in a viscous medium. Curves are obtained using the Malvern general purpose scattered intensity-weighted diffusion coefficient distribution analysis (non-negative least squares (NNLS)). The arrow indicates a consistent shift in peak diffusion with increasing H_2O_2.

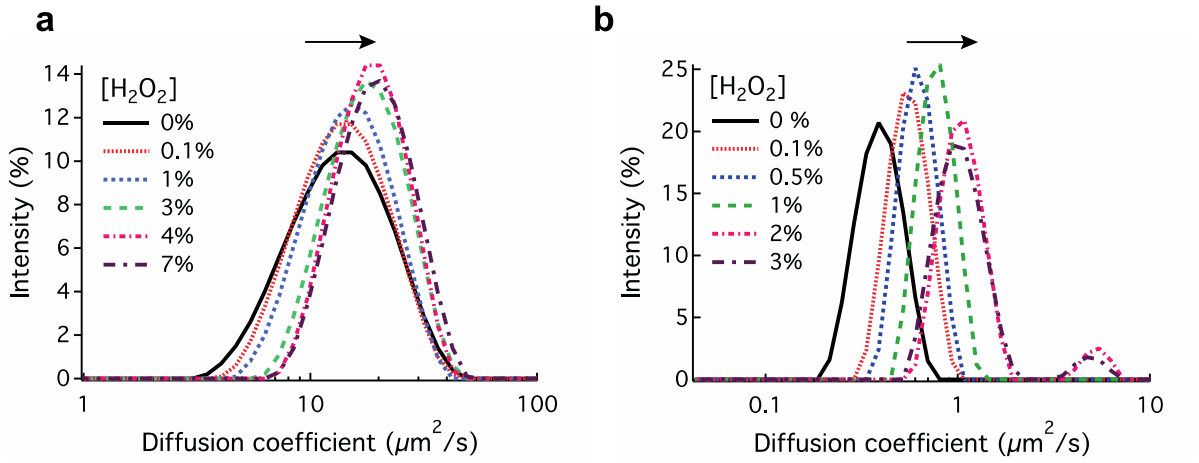

SI- Figure 7| DLS autocorrelation functions and diffusion coefficient distributions in H_2O_2 for: **(a)** Au NP (red) and control solution of Au NP physically mixed with reduced Pt with 2% (v/v) H_2O_2 (dashed black) and without (solid black); **(b)** thick layer core-shell Pt-Au NP with 0.1% (v/v) H_2O_2 (red) and without (solid black). Measurements at higher fuel concentrations were impractical as a result of oxygen bubble formation caused by the high catalytic activity of these particles. An erroneous autocorrelation function is shown (dashed line) is shown in part b as an example of invalid data affected by bubble formation or aggregation; such does not meet the quality criteria and is removed from the analysis. Neither sample shows evidence of a significant increase in apparent diffusivity on addition of fuel.

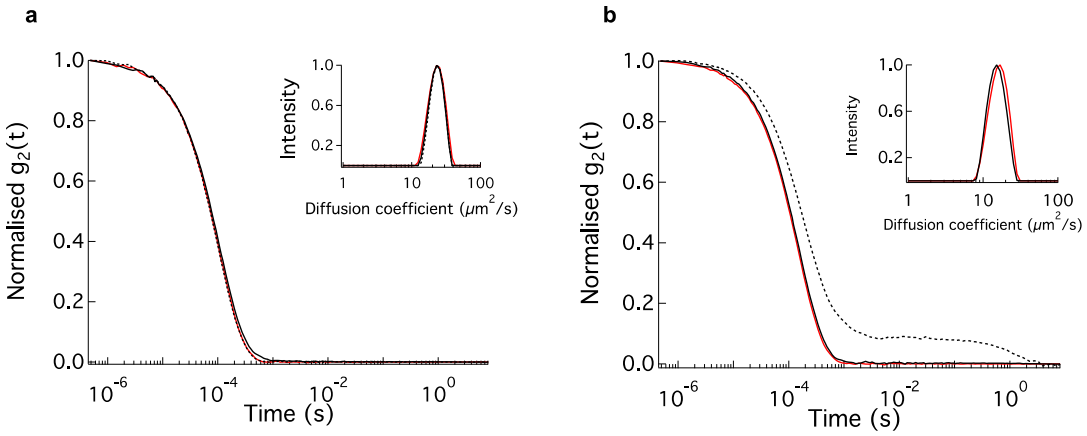

SI- Figure 8 DLS diffusion measurement of 5 nm Pt NP in viscous solution.

The diffusion coefficient for 5 nm Pt NP (in units of D_0=0.87μm^{2}s^{-1}) is plotted as a function of H_2O_2 concentration, averaged over 3 experimental runs (error bars indicate standard deviations). A *decrease* of 40% in diffusivity in 2% (v/v) H_2O_2 is observed. A similar observation has been reported[1] for 30 nm Pt NP in water; this was attributed to a slight increase in viscosity in the presence of H_2O_2. While viscosity does increase with H_2O_2 concentration, the magnitude of the change (1.01 cP for 8% (m/m) H_2O_2 vs. 1.001 cP for H_2O at 20 ^oC)[2] is insufficient to account for the measured change in diffusivity. The apparent decrease of diffusivity may result from the accumulation of gaseous oxygen around the Pt NP.

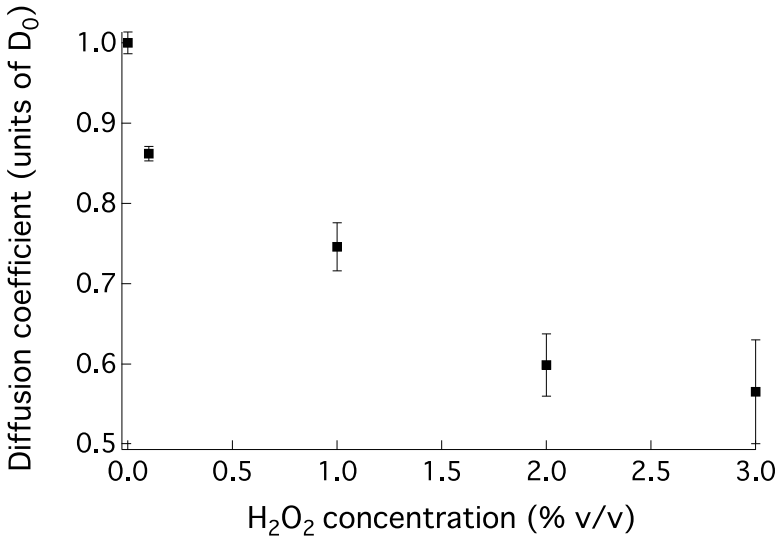

References

1 T.-C. Lee, M. Alarcón-Correa, C. Miksch, K. Hahn, J. G. Gibbs and P. Fischer, *Nano Lett.*, 2014, **14**, 2407–2412.

2 M. K. Phibbs and P. A. Giguère, *Can. J. Chem.*, 1951, **29**, 173–181.